inter-noise 2002

The 2002 International Congress and Exposition on Noise Control Engineering
Dearborn, MI, USA. August 19-21, 2002

Analysis of Friction-Induced Vibration Leading to Eek Noise in a Dry Friction Clutch

P. Wickramarachi* and R. Singh
Acoustics and Dynamics Laboratory, Center for Automotive Research
The Ohio State University, Columbus, Ohio 43210-1107, USA

G. Bailey
LuK, Inc., 3401 Old Airport Road - Wooster Ohio 44691, USA

Abstract

This study deals with a severe noise problem (Eek) that arises during the engagement of a dry friction clutch in a vehicle with manual transmission. Measurements have shown that near the full engagement the pressure plate suddenly starts vibrating (rigid body wobbling mode) with a frequency close to the first natural frequency of the rotational sub-system. This self-excited vibration problem exhibits typical signs of a dynamic instability associated with a constant friction coefficient. The transient event results in the generation of high transient noise levels and often consumers will change clutches prematurely in an effort to eliminate this noise. Our work focuses on developing a linearized lumped-parameter model of the clutch. The effect of key parameters on the system stability is examined by calculating complex eigensolutions. Results of this analytical study are in agreement with experimental observations. It is seen that the instability of the rigid body wobbling mode is controlled by the friction forces. This mode may, however, be also affected by the first bending mode of the pressure plate. Therefore, a stiffer plate could lead to a design with a reduced tendency to Eek.

1. Introduction

A strong squealing noise is produced during the engagement of a dry friction clutch in a manual transmission. This is known as “Eek” noise and it dictates the overall perception of vehicle quality. Despite many experimental studies, this friction-induced phenomenon remains poorly understood. One hypothesis is that Eek is triggered by a dynamic instability of the system composed of the pressure plate and the disc cushion. It has been experimentally observed that, during the Eek event, the pressure plate vibrates in a rigid body wobbling motion at the natural frequency of the rotational system (out of plane). This is correlated with

* Currently with Data Physics Corporation, <wickramarachi@dataphysics.com>

a Single-Degree-Of-Freedom model (SDOF) that includes the pressure plate inertia, the diaphragm spring stiffness, and the cushion stiffness only. In addition, experimental studies show that the modal properties of the pressure plate itself, due to the fabrication process, seem to play a significant role in the Eek mechanism(s). To clarify some of these issues, we develop an analytical model that could be used to identify key parameters affecting the system stability. Based on experimental modal analyses (though not presented here), the complex eigenvalue method is applied to a linearized lumped-parameter model. It is used to demonstrate the potential coupling between the pressure plate-wobbling mode and the first elastic deformation mode of the pressure plate. Then stability maps are developed in terms of the friction coefficient and the pressure plate geometry and structural stiffness.

2. Problem Formulation

Two conditions are typically necessary to generate the transient Eek noise (Figure 1). First, the engine speed should be within the 1500-2500 RPM range. Conversely, the transmission speed does not seem to have a significant effect. Since the slip speed is relatively high, one may assume a constant coefficient of friction μ at the threshold of Eek. This shows that the Eek noise may not follow the symptoms of classical stick-slip phenomena [1]. Second, the clutch pedal motion (bearing travel) must be such that the clutch is close to full engagement. Observe this particular position (where Eek begins to occur) in Figure 1 and note that the pressure plate and the disc cushion are already in contact. Measurements of noise spectra exhibit a dominant frequency f_w, which is related to the bearing travel, around 450 Hz (Figure 2.1). This frequency has been correlated to the wobbling rigid body motion of the pressure plate (both out-of-plane rotations) from dynamometer tests and the SDOF model. Therefore the pressure plate and the disc cushion are assumed to be the main components that control the Eek phenomenon. This observation is reinforced by many experiments as elements external to the clutch (gears, release system, engine pulsations, etc.) and internal to the clutch (diaphragm spring and cover) have not significantly influenced the tendency to Eek [2].

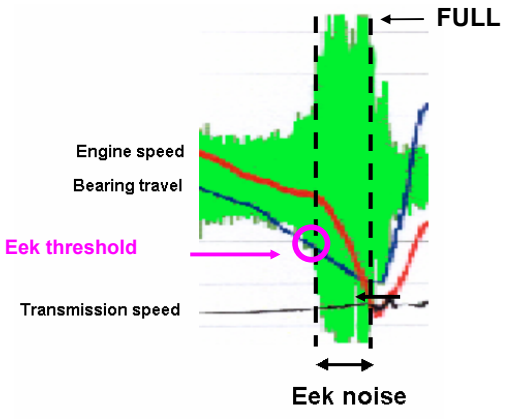

Figure 1: Eek noise measurement (in-vehicle)

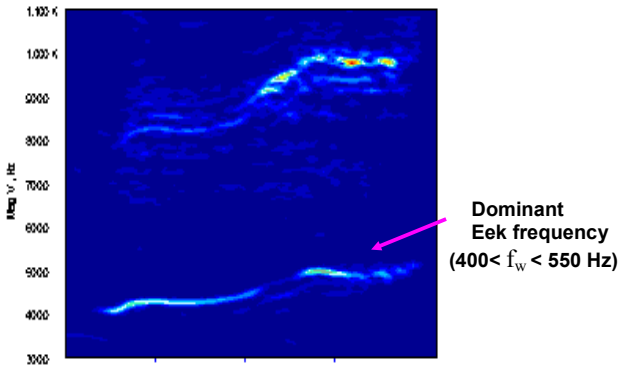

Figure 2.1: Time-frequency diagram

However, a change in the pressure plate material from gray-iron (Plate G) to vermicular iron (Plate V) seems to reduce the occurrence of Eek. Such a change could alter the modal properties of the pressure plate, as reported in some brake-squeal studies [4]. Hence, we need to investigate the influence of the pressure plate elastic deformations. From experimental modal analyses, the second frequency f_b (≈ 900 Hz) of Figure 2.1 could be linked to the first bending mode of the plate. Observe the presence of this mode (f_b) at t = 2.8 s in Figure 2.2, which is quickly replaced by the wobbling mode (f_w and harmonics) at t = 3.1 s in Figure 2.3. Our study will then attempt to develop a preliminary simulation model of the clutch. At the threshold of Eek, vibration amplitudes are considered sufficiently small to build a linearized model that could reproduce the trends of observed dynamic instabilities. Here, the lumped parameter approach is preferred over the FE method. Our study examines a self-excited system, without any external torque excitations. Moreover, our model will demonstrate a possible coupling between the rigid body-wobbling mode and the first bending mode of the pressure plate. The pressure plate is assigned an initial angle in order to inspect the amplitude growth with time and demonstrate the existence of dynamic instability.

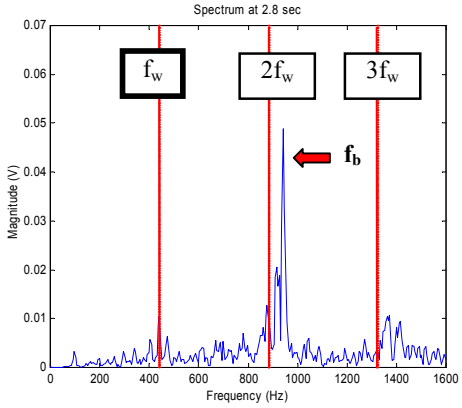

Figure 2.2: Spectrum at t = 2.8 sec (mode at f_b)

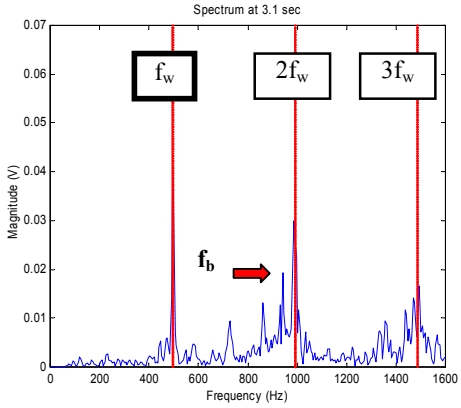

Figure 2.3: Spectrum at t = 3.1 sec (mode at f_w)

3. Lumped Parameter Model

The lumped parameter model of Figure 3 incorporates the inertia of a deformable pressure plate along with the cushion stiffness k_c that is split into four springs of stiffnesses k_{xf}, k_{xr}, k_{yf} and k_{yr} . In order to consider the nonlinear characteristic of the cushion, the stiffnesses k_{yf} and k_{yr} are respectively divided and multiplied by a ratio γ, as explained in Figure 4 and the following. Assume that the bearing travel is such that the Eek threshold point (point P) is reached. This would correspond to a plate liftoff $\upsilon = \upsilon_{eek}$. Now suppose that the plate is already vibrating about the x-axis with amplitude θ_{xo}. This will change the normal spring forces at locations A and B and consequently the stiffnesses k_{yf} and k_{yr} by assuming a constant stiffness slope around point P, as shown by Equation 1.

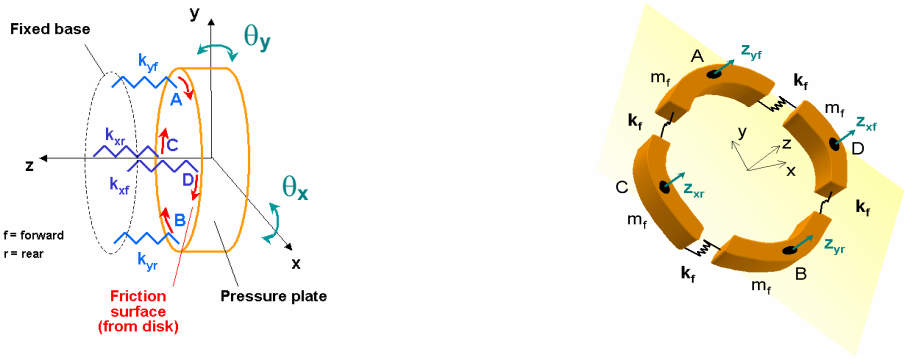

Figure 3: Lumped-parameter model, (a) 2 rotational DOFs θ_x and θ_y, (b) 4 translational DOFs in z direction

$$k_{yr} = \frac{k_c}{4\gamma} \qquad \text{where } \gamma = 0.9 \qquad (1)$$

$$k_{yf} = \gamma \frac{k_c}{4}$$

The friction forces from the cushion are also included by assuming a constant μ due to high slip speeds (>700 RPM). In terms of the Degrees-Of-Freedom (DOFs), this model is composed of two DOFs corresponding to the rigid body "out-of-plane" rotations (wobbling mode) and four additional translational DOFs (normal to the pressure plate) to incorporate the first 2-nodal diameter mode of the pressure plate. By choosing appropriate lumped bending stiffnesses k_f, we estimate the frequency of this bending mode to be close to f_b. The value m_f corresponds to a quarter of the total plate mass.

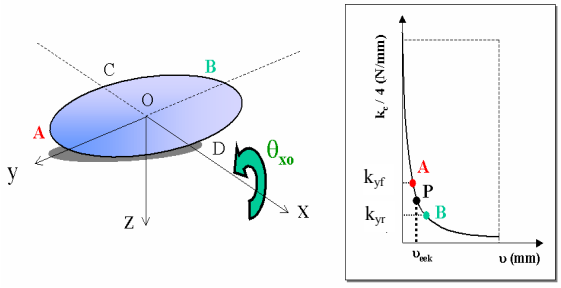

Figure 4: Modeling of cushion nonlinear effect

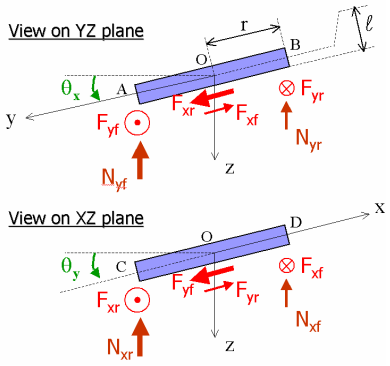

Figure 5: Free-body diagrams

Next, the free-body diagrams are drawn in Figure 5. Here, even though the plate is represented as a rigid body for the sake of clarity, it can also elastically deform as explained before. The normal spring forces and the corresponding friction forces are expressed as:

$$
\begin{aligned}
N_{xf} &= k_{xf}(z - r\theta_y) & F_{xf} &= \mu N_{xf} \\
N_{xr} &= k_{xr}(z + r\theta_y) & F_{xr} &= \mu N_{xr} \\
N_{yf} &= k_{yf}(z + r\theta_x) & F_{yf} &= \mu N_{yf} \\
N_{yr} &= k_{yr}(z - r\theta_x) & F_{yr} &= \mu N_{yr}
\end{aligned}
\tag{2}
$$

The resulting governing equations for the linear, undamped and unforced system are obtained in terms of the mass [M] and stiffness [K] matrices and the generalized coordinate vector $\{X\}$.

$$
[M]\{\ddot{X}\} + [K]\{X\} = \{0\} \tag{3}
$$

where $X^T = [\theta_x \quad \theta_y \quad z_{xf} \quad z_{xr} \quad z_{yf} \quad z_{yr}]^T$, $M = diag([I_x \quad I_y \quad m_f \quad m_f \quad m_f \quad m_f])$

$$
K = \begin{bmatrix}
r^2(k_{yf}+k_{yr}) & \mu r(k_{xf}+k_{xr}) & -G_{xf} & -G_{xr} & r(2k_f+k_{yf}) & -r(k_{yr}-2k_f) \\
-\mu r(k_{yf}+k_{yr}) & r^2(k_{xf}+k_{xr}) & -r(k_{xf}-2k_f) & r(2k_f+k_{xr}) & -G_{yf} & -G_{yr} \\
0 & -rk_{xf} & 2k_f+k_{xf} & 0 & -k_f & -k_f \\
0 & rk_{xr} & 0 & 2k_f+k_{xr} & -k_f & -k_f \\
rk_{yf} & 0 & -k_f & -k_f & 2k_f+k_{yf} & 0 \\
-rk_{yr} & 0 & -k_f & -k_f & 0 & 2k_f+k_{yr}
\end{bmatrix}
$$

, $G_{ij} = f(\mu, r, \ell, k_f, k_{ij})$, for $i=\{x,y\}$, $j=\{f,r\}$

4. Stability Studies and Design Maps

The asymmetric nature of [K], as controlled by μ and γ, yields complex eigenvalues $\lambda_k = \sigma_k \pm \omega_k$, where the imaginary part ω_k is the frequency of mode k (in rad/s) and the real part σ_k is an index of stability. When σ_k is positive, the amplitude of vibration grows exponentially in time. The effect of μ on λ_k is examined in Figure 6. Observe two distinct wobbling modes with frequencies f_1 and f_2 (in Hz), where the frequency gap is found to be related to the ratio γ for low values of μ. Nevertheless, as μ is increased, so is the coupling between those two modes. It results in stable and unstable modes occurring at the same frequency f_c. This would occur when $\mu = 0.35$, which is typical for disc linings. Next, the effect of the pressure plate structural stiffness k_f is investigated in Figure 7, which maps the frequencies and real parts of the wobbling modes. As k_f is increased, one passes from an unstable region (for Plate G) to a stable region (for Plate V). This observation is in agreement with measurements and experimental modal analyses that show that Plate V is essentially stiffer than Plate G. Therefore, the Young's modulus does have a significant impact on the system stability and on Eek noise.

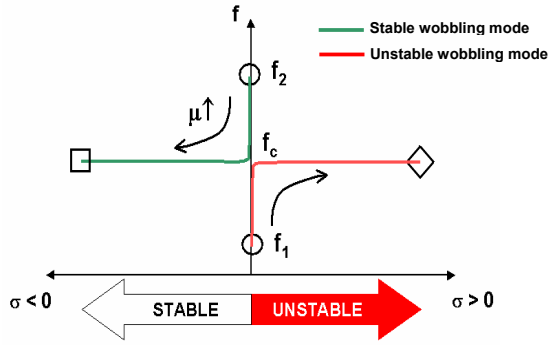

Figure 6: Predicted eigenvalues with varying μ

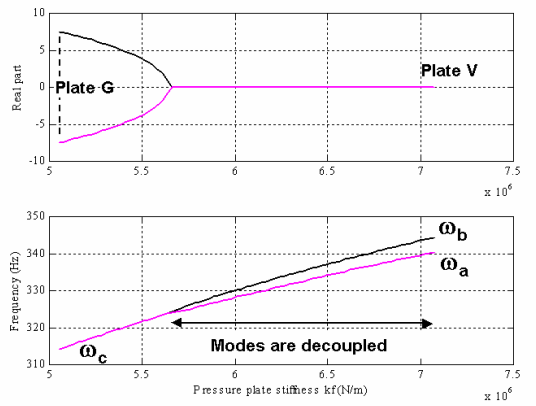

Figure 7: Predicted eigenvalues with varying k_f

Next, an animation of complex wobbling modes is developed to visualize phase differences (such as Figure 8). As the pressure plate wobbles, a circle indicates the location along the edge that has the maximum positive amplitude (z-direction). At $\mu = 0.35$, this circle actually moves along the edge in the direction of the friction forces for the unstable mode (represented by the eigenvector ψ_1) and in the opposite direction for a stable mode (ψ_2). This means that the axis of rotation (dash line) is actually rotating as a function of time and in a different direction as shown in this figure. Hence, the friction forces may enhance energy of an unstable mode, while they may dissipate energy of a stable mode. At lower μ values, the axis of rotation remains stationary, which shows the absence of any coupling between θ_x and θ_y.

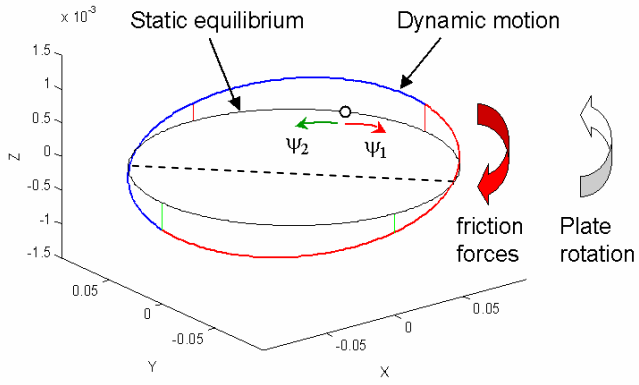

Figure 8: Animation of complex wobbling modes for $\mu = 0.35$, showing the directions of the traveling waves induced by ψ_1 and ψ_2 (moving axis of rotation)

Stability maps are presented next as they reveal the effects of pressure plate geometry (inner and outer radii r_i and r_o, and thickness 2ℓ), pressure plate structural stiffness (k_f) and disc cushion characteristics (μ and k_c). First, a map in terms of r_i and r_o is displayed in Figure 9. Defining $\delta = 0.5(r_o - r_i)$, the radii are varied from their baseline value minus δ to their baseline value plus δ. The increasing levels of instability are represented with a color code. Two straight lines indicate the baseline values. It is found that larger radii would result in an

increased stability. However, r_o seems to have a greater influence than r_i. For practical purposes, it would be more suitable to maintain the same contact area between the pressure plate and the disc. A smaller surface is not recommended since it would produce more heat and reduce the clutch life. Note that the heat capacity of the clutch is also affected by the pressure plate mass. From these considerations, it seems that r_o is the parameter that should be increased, since a 15% increase would theoretically result in a stable system. In addition, this change would increase the torque capacity of the clutch.

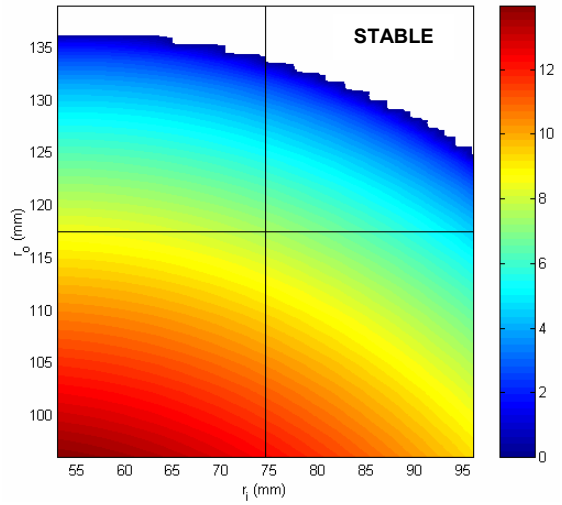

Figure 9: Stability map with varying r_i and r_o

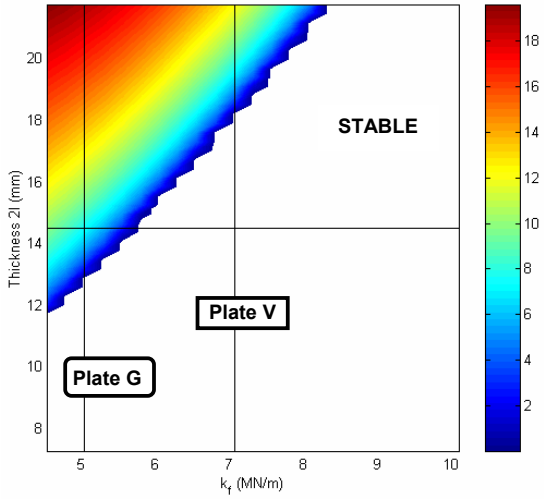

Figure 10: Stability map with varying ℓ and k_f

Second, the stability map of Figure 10 shows that a thicker pressure plate would result in a decrease of stability. This is conceivable since ℓ controls the torque generated by the friction forces (recall Figure 5). This torque is responsible for the wobbling mode, because it couples θ_x with θ_y. Interestingly a 10% decrease in ℓ would make the system stable. As with the previous design change proposed for r_o, one needs to consider the consequences of a thinner plate in terms of clutch life and performance. For example, a change in ℓ would affect k_f, which is related to the bending mode of the pressure plate. The next map (Figure 11) compares the influence of μ on plates G and V. Note that plate V is stable for $\mu < 0.45$. As for plate G, decreasing μ by 10% (0.35 to 0.31) would make the system stable. Once again, this change may cause problems in terms of the clutch performance, since the transmitted torque would be also reduced. To compensate, the clamp load (normal load at full engagement) would have to be increased accordingly. Finally, a stability map is obtained in terms of k_f and k_c, in Figure 12. The latter is varied up to its maximum value at full engagement. In parallel, the eigenvalues are computed via an iterative process to get the corresponding values for k_{yr} and k_{yf} at each point on the plot. Figure 9 shows the loss of stability as the clutch is being engaged. Here it occurs around $k_c \approx 26$ MN/m for plate G, whereas the instability region is avoided with plate V at the same value. Such predictions match experimental observations fairly well.

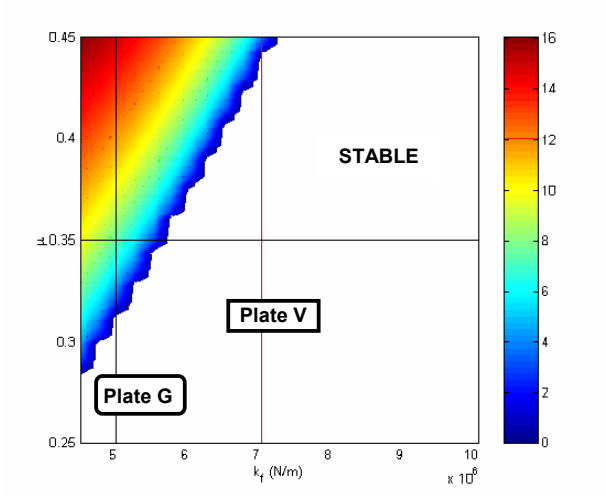

Figure 11: Stability map with varying μ and k_f

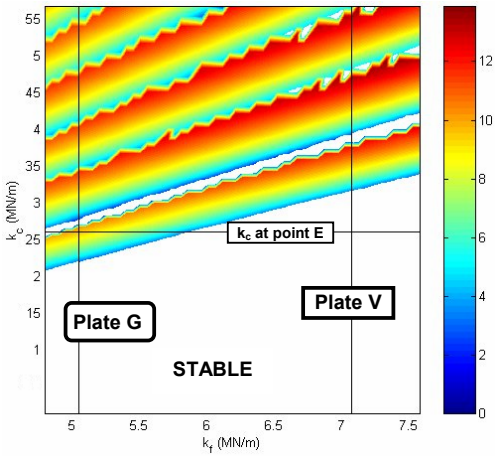

Figure 12: Stability map simulating a clutch engagement with varying k_f

5. Conclusion

The simulation study has given us some insights into the mechanism(s) of Eek noise in clutches. Specifically, the friction-induced vibration of the pressure plate-disc cushion system has been correlated with a loss of dynamic stability. Our models describe a 6-DOF lumped-parameter system, and we include both rigid body wobbling mode and first elastic deformation mode of the plate. The complex eigenvalue method is then utilized to map the system stability in terms of the friction coefficient, pressure plate geometry and structural stiffness of the pressure plate. The latter is found to be a key parameter. By controlling the frequency of the first elastic deformation mode, we can alter the coupling with the wobbling mode. This instability mechanism and its effect are correlated with experimental observations. Future work should focus on developing a more analytical basis for the Eek phenomena.

Acknowledgements

We thank Dr. Todd Rook of BFGoodrich and the engineering team at LuK, Inc, for their valuable help in solving parts of the Eek mystery.

References

1. A. J. McMillan, A Non-linear Friction Model for Self-excited Vibrations, *Journal of Sound and Vibration* 205(3), 323-335, 1997.
2. Discussions with LuK, Inc. engineers, 2000-2001.
3. S. W. Kung, K. B. Dunlap and R. S. Ballinger, Complex Eigenvalue Analysis for Reducing Low Frequency Brake Squeal, *SAE paper* # 2000-01-0444.
4. D. J. Feld and D. J. Fehr, Complex Eigenvalue Analysis Applied to an Aircraft Brake Vibration Problem, *ASME Design Engineering Technical Conferences*, DE-Vol 84-1, Volume 3 – Part A, 1995.